Protein kinase C is a calcium sensor for presynaptic short-term plasticity

(Article begins on next page)

Protein kinase C is a calcium sensor for presynaptic short-term plasticity

Diasynou Fioravante[1,2†], YunXiang Chu[1†], Arthur PH de Jong[1], Michael Leitges[3], Pascal S Kaeser[1], Wade G Regehr[1]*

[1]Department of Neurobiology, Harvard Medical School, Boston, United States; [2]Center for Neuroscience, University of California, Davis, Davis, United States; [3]The Biotechnology Center of Oslo, University of Oslo, Oslo, Norway

Abstract In presynaptic boutons, calcium (Ca^{2+}) triggers both neurotransmitter release and short-term synaptic plasticity. Whereas synaptotagmins are known to mediate vesicle fusion through binding of high local Ca^{2+} to their C2 domains, the proteins that sense smaller global Ca^{2+} increases to produce short-term plasticity have remained elusive. Here, we identify a Ca^{2+} sensor for post-tetanic potentiation (PTP), a form of plasticity thought to underlie short-term memory. We find that at the functionally mature calyx of Held synapse the Ca^{2+}-dependent protein kinase C isoforms α and β are necessary for PTP, and the expression of PKCβ in PKCαβ double knockout mice rescues PTP. Disruption of Ca^{2+} binding to the PKCβ C2 domain specifically prevents PTP without impairing other PKCβ-dependent forms of synaptic enhancement. We conclude that different C2-domain-containing presynaptic proteins are engaged by different Ca^{2+} signals, and that Ca^{2+} increases evoked by tetanic stimulation are sensed by PKCβ to produce PTP.

DOI: 10.7554/eLife.03011.001

*For correspondence: wade_regehr@hms.harvard.edu

†These authors contributed equally to this work

Introduction

The complex manner in which patterns of action potentials (AP) are transformed into neurotransmitter release suggests the existence of multiple presynaptic calcium (Ca^{2+}) sensors (***Kaeser and Regehr, 2013***). Synaptotagmin-1, synaptotagmin-2, and synaptotagmin-9 have been identified as Ca^{2+} sensors for synchronous release (***Sudhof, 2013***), but the Ca^{2+} sensors that regulate short-term use-dependent plasticity remain elusive. For a widespread form of short-term plasticity termed post-tetanic potentiation (PTP), a high-frequency burst of presynaptic APs enhances subsequent AP-evoked release for tens of seconds. PTP requires sustained elevation of presynaptic Ca^{2+}, and in most cases synaptic enhancement outlives Ca^{2+} increases (***Regehr et al., 1994***; ***Brager et al., 2003***; ***Korogod et al., 2005***; ***Habets and Borst, 2007***; ***Fioravante et al., 2011***, ***2012***). Although PTP is thought to contribute to short-term memory (***Silva et al., 1996***; ***Abbott and Regehr, 2004***), the Ca^{2+} sensor that mediates this plasticity has not been identified.

Three Ca^{2+}-dependent isoforms of protein kinase C (PKC_{Ca}; PKCα, PKCβ, and PKCγ) play crucial roles in PTP (***Fioravante et al., 2011***, ***2012***; ***Chu et al., 2014***). Because these isoforms contain Ca^{2+}-binding C2 domains (***Shao et al., 1996***; ***Sutton and Sprang, 1998***), we hypothesize that they function as Ca^{2+} sensors for PTP. However, it is unclear whether the Ca^{2+}-binding properties of the C2 domain of PKC_{Ca} (***Kohout et al., 2002***) are well-suited to mediate PTP, which is thought to rely, at least in part, on the waning residual Ca^{2+} after the AP burst (***Fioravante and Regehr, 2011***). Moreover, diacylglycerol (DAG) binding to the C1 domain of PKC_{Ca} (**Figure 1A**) can regulate the activity of PKC_{Ca} (***Newton, 2010***), and it has been proposed that PKC could play a permissive role in PTP rather than function as the Ca^{2+} sensor (***Saitoh et al., 2001***). Indeed, presynaptic C2-domain proteins do not necessarily function as Ca^{2+} sensors; rather, they can regulate release independent of their Ca^{2+}-binding properties (for an example, see ***Groffen et al., 2010***; ***Pang et al., 2011***). Furthermore, additional Ca^{2+}-binding

eLife digest Brain function is dependent upon the rapid transfer of information from one brain cell to the next at junctions known as synapses. When an electrical signal called an action potential is generated by the cell before the synapse, the presynaptic cell, it triggers an influx of calcium ions into that cell. These ions activate specific calcium sensors, triggering release of molecules called neurotransmitters from the presynaptic cell through exocytosis of synaptic vesicles. These neurotransmitters bind to receptors on the membrane of the postsynaptic cell, and produce an electrical signal whose size is a measure of synaptic strength.

The strength of a synapse can change over time—a property that is called plasticity. Synapses can undergo both long-term and short-term increases in strength. Post-tetanic potentiation is a short-term increase in strength that lasts for tens of seconds: it is triggered by a calcium increase in the presynaptic cell and involves an increase in the amount of neurotransmitter released in response to each presynaptic action potential. Post-tetanic potentiation is thought to underlie short-term memory. However, the identity of the sensor that detects the build-up of calcium in post-tetanic potentiation was not known.

Now, Fioravante, Chu et al. have provided the first direct evidence that an enzyme called protein kinase C is responsible. Electrophysiological recordings in brain slices from genetically modified mice revealed that animals that lack protein kinase C do not show post-tetanic potentiation. However, potentiation can be restored by re-introducing the enzyme into presynaptic cells. Importantly, a mutated version of protein kinase C that lacks the ability to bind calcium is unable to trigger post-tetanic potentiation.

Protein kinase C represents a new class of presynaptic calcium sensors that supports short-term plasticity. It is likely that future studies will identify additional members of this class of sensors that allow different synapses to have different forms of short-term plasticity. Further research is also needed to clarify the mechanisms underlying short-term plasticity and to understand how different forms of short-term plasticity are associated with different functions and behaviors.

DOI: 10.7554/eLife.03011.002

proteins have been implicated in short-term plasticity (*Sakaba and Neher, 2001*; *Junge et al., 2004*; *Mochida et al., 2008*; *He et al., 2009*; *Shin et al., 2010*), but it has not been established that Ca^{2+} binding to these proteins is required for short-term plasticity. Thus, in order to determine whether PKC_{Ca} isoforms are Ca^{2+} sensors that mediate PTP, it must be determined if PTP relies on Ca^{2+} binding to the PKC_{Ca} C2 domain.

Results

To investigate the function of PKC_{Ca} isoforms in PTP, we first examined their role at the functionally mature calyx of Held synapse (postnatal day 17–22) (*Fedchyshyn and Wang, 2005*; *Yang et al., 2010*) using double knockout mice for PKCα and β (αβ dko). We recorded excitatory postsynaptic currents (EPSCs) from principal neurons in the medial nucleus of the trapezoid body (MNTB) in response to extracellular stimulation. Tetanic stimulation induced PTP in wild-type animals (*Figure 1B*, *black*) but not in PKCαβ dko animals (*Figure 1B*, *purple*). Thus, in contrast to the immature calyx of Held where a substantial component of PTP (~20%) is independent of PKC_{Ca} (*Fioravante et al., 2011*), PTP at the functionally mature calyx of Held relies entirely on PKC_{Ca} isoforms.

We further tested whether the contribution of PKC_{Ca} to a related form of potentiation that occludes PTP also increases with development. Phorbol 12,13-dibutyrate (PDBu), a DAG analog, can enhance transmission by activating not only PKC_{Ca} (*Figure 1A*) but also Ca^{2+}-insensitive PKC isoforms and other presynaptic proteins (*Brose and Rosenmund, 2002*; *Newton, 2010*). At immature calyces, ~35% of PDBu-mediated enhancement is independent of PKC_{Ca} (*Fioravante et al., 2011*). We found that PDBu enhances release at functionally mature wild-type calyces (*Figure 1C*, *black*) but not at age-matched αβ dko calyces (*Figure 1C*, *purple*). Thus, at the functionally mature calyx of Held, both PTP and PDBu-mediated enhancement rely entirely on PKC_{Ca}, suggesting that the contributions of parallel mechanisms to these forms of plasticity (e.g., *Wierda et al., 2007*; *Shin et al., 2010*) diminish with development.
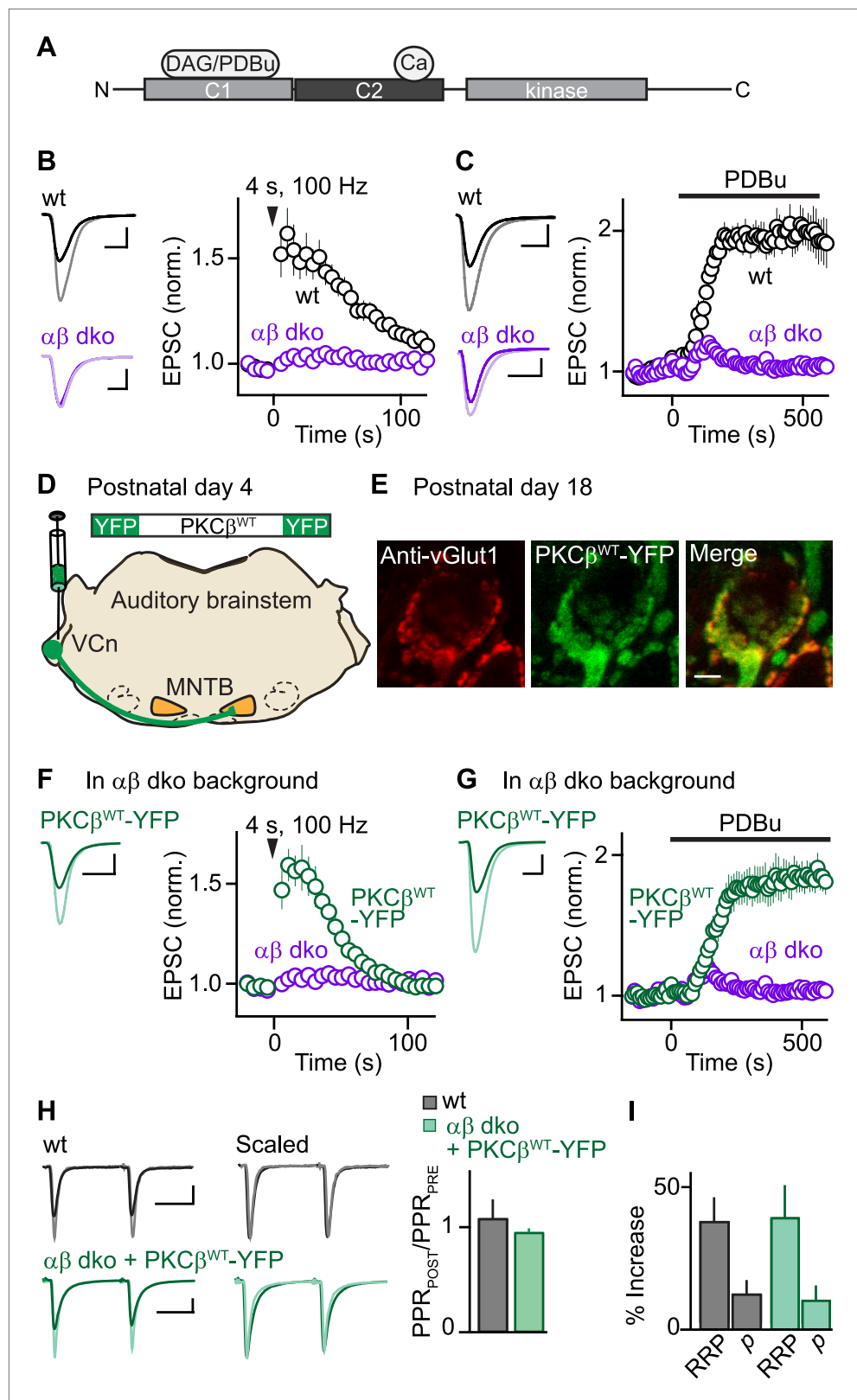
Figure 1. Expression of PKCβ rescues synaptic potentiation in animals lacking calcium-dependent PKCs. Synaptic plasticity was examined at the calyx of Held following tetanic stimulation (**B** and **F**) or bath application of the phorbol ester PDBu (**C** and **G**) for wild-type (wt, *black*), PKCαβ dko animals (*purple*), and PKCαβ dko animals
Figure 1. Continued on next page

Figure 1. Continued

expressing PKCβ[WT]-YFP (*green*). (**A**) Domain arrangement of PKC$_{Ca}$. DAG and PDBu bind to the C1 domain and Ca^{2+} binds to the C2 domain. (**B**, **C**, **F**, **G**) Left, example EPSCs recorded prior to (*bold traces*) and after (*light traces*) synaptic enhancement for each experimental condition. Right, EPSCs are plotted as a function of time (mean ± SEM). For (**B**), wild-type: 62 ± 12%; αβ dko: 2.4 ± 1.8%. Also see *Figure 1—figure supplement 1* and accompanying legend for PTP induced under elevated-temperature conditions. Similar to PTP induced at room temperature, PTP at near-physiological temperature requires PKC$_{Ca}$ (*Figure 1—figure supplement 2*). For (**C**), at steady state: wild-type: 97 ± 12%; αβ dko: 3.2 ± 3.4%; for (**F**), PKCβ[WT]-YFP: 61 ± 7%; for (**G**), 84 ± 11%. In **F** and **G**, the αβ dko group data from **B** and **C** respectively are re-plotted for comparison. Also see *Figure 1—figure supplement 3* and *Figure 1—figure supplement 4*. (**D**) In this schematic of the auditory brainstem, the ventral cochlear nucleus (VCn) and medial nuclei of the trapezoid body (MNTB) are labeled. An AAV expressing PKCβ[WT]-YFP was injected in the VCn at postnatal day 4. (**E**) Confocal images of a brain section labeled with an antibody against vGlut1 (*red*) are shown for a calyx of Held expressing PKCβ[WT]-YFP (*green*) in a PKCαβ dko animal at postnatal day 18. Scale bar: 10 μm. (**H** and **I**) The synaptic mechanism through which PKCβ rescues PTP was examined under conditions that relieve AMPA receptor desensitization and saturation. (**H**) Left, overlay of EPSCs (10 ms inter-stimulus interval) delivered prior to (*bold traces*) and 10 s after (*light traces*) PTP-inducing tetanus. Middle, traces are normalized to the first EPSC to allow comparison of PPR. Right, PPR$_{POST}$ (after tetanus) over PPR$_{PRE}$ (before tetanus) (mean ± SEM, see *Figure 1—source data 1 and 2*). Wild-type: p=0.49; αβ dko expressing PKCβ[WT]-YFP: p=0.68. (**I**) Summary of the readily releasable pool (RRP) and release probability (*p*) contributions to PTP (mean ± SEM, also see *Figure 1—figure supplements 5 and 6* and *Figure 1—source data 1 and 2*). RRP$_{WT}$: 37 ± 9%; RRP$_{PKCβWT-YFP}$: 39 ± 12%; p=0.88. Scale bars in **B**, **C**, **F**, and **G**: 2 nA, 1 ms. Scale bars in **H**: 2 nA, 5 ms.
DOI: 10.7554/eLife.03011.003

The following source data and figure supplements are available for figure 1:

Source data 1. Summary and statistical analyses of synaptic properties during PTP and PDBu-induced potentiation.
DOI: 10.7554/eLife.03011.004

Source data 2. Summary and statistical analyses of basal synaptic properties.
DOI: 10.7554/eLife.03011.005

Figure supplement 1. PTP can be induced under near-physiological conditions.
DOI: 10.7554/eLife.03011.006

Figure supplement 2. Under near-physiological conditions PTP is mediated by PKC$_{Ca}$.
DOI: 10.7554/eLife.03011.007

Figure supplement 3. At the functionally mature calyx of Held, PKCα does not contribute to PTP but plays a small role in phorbol ester-induced potentiation.
DOI: 10.7554/eLife.03011.008

Figure supplement 4. PKC$_{Ca}$ isoforms do not regulate basal synaptic properties.
DOI: 10.7554/eLife.03011.009

Figure supplement 5. Determining the contributions of RRP and *p* in wild-type and rescued PTP at the functionally mature calyx of Held.
DOI: 10.7554/eLife.03011.010

Figure supplement 6. Determining the contributions of RRP and *p* in wild-type and rescued PTP at the functionally mature calyx of Held.
DOI: 10.7554/eLife.03011.011

Although most of the studies presented here were performed at room temperature, we also examined PTP at near-physiological temperatures (34°C). Higher stimulus frequencies were required to induce PTP (*Figure 1—figure supplement 1*), but PTP was still dependent on PKC$_{Ca}$ (*Figure 1—figure supplement 2*).

We next assessed whether presynaptic expression of PKCβ in αβ dko animals rescues PTP. PKCβ was chosen because genetic deletion of PKCα had little effect on PTP (*Figure 1—figure supplement 3*), suggesting that PTP is mediated primarily by PKCβ at the functionally mature calyx. We generated an adeno-associated virus (AAV), which we used to express wild-type PKCβ fused to yellow fluorescent protein (PKCβ[WT]-YFP) in αβ dko animals (*Figure 1D*). Two weeks after injection, virally expressed PKCβ[WT]-YFP localized to glutamatergic terminals positive for the marker vGlut1 (*Figure 1E*). In contrast to non-injected αβ dko animals, we observed reliable PTP at synapses expressing PKCβ[WT]-YFP (*Figure 1F*, *green*; compare to non-injected age-matched αβ dko animals, *purple*). Expression of PKCβ[WT]-YFP did not alter basal synaptic properties (*Figure 1—figure supplement 4*). Moreover, PKCβ[WT]-YFP

expression supported PDBu-induced potentiation in αβ dko mice (*Figure 1G*, *green*), which was very similar in amplitude to that observed in wild-type animals (*Figure 1C*, *black*; *Figure 1—source data 1*). Thus, expression of PKCβ is sufficient to rescue PTP and PDBu-mediated enhancement in PKC αβ dko animals.

To determine whether rescued PTP and PTP in wild-type animals are mediated by the same synaptic mechanism, we calculated the paired-pulse ratios (PPR = EPSC2/EPSC1) before and at the peak of PTP. If PTP reflects an increase in vesicular release probability (p), which is inversely related to PPR, then PPR_{POST}/PPR_{PRE} should decrease. However, PPR_{POST}/PPR_{PRE} was unchanged in both wild-type (*Figure 1H*, *black*) and αβ dko animals expressing $PKCβ^{WT}$-YFP (*Figure 1H*, *green*). This suggests that in both groups PTP is not mediated by an increase in p. We next examined the contribution of the readily releasable pool (RRP) of vesicles to PTP by evoking EPSCs with AP trains before and at the peak of PTP (*Figure 1—figure supplement 5*) and found that PTP was mediated by equivalent increases in the RRP in wild-type and rescued groups (*Figure 1I*, *Figure 1—figure supplement 6*). Thus, at the functionally mature calyx, the same mechanism mediates PTP in wild-type animals and at synapses in PKCαβ dko animals that express $PKCβ^{WT}$-YFP.

To determine if PKCβ is the Ca^{2+} sensor for PTP, it is necessary to abolish Ca^{2+} binding to PKCβ. To this end, we mutated five C2-domain aspartates (D) to alanines (A) and examined the effect on Ca^{2+} binding using purified recombinant wild-type C2 ($C2^{WT}$) and mutant $C2^{D/A}$ domains (*Figure 2A,B*, *Figure 2—figure supplement 1*). These aspartates are predicted to mediate Ca^{2+} binding based on structural similarity (*Nalefski and Falke, 1996*; *Ubach et al., 1998*). We assessed Ca^{2+} binding through changes in intrinsic fluorescence of tryptophan residues adjacent to the predicted Ca^{2+}-binding sites (*Figure 2—figure supplement 1*; *Nalefski and Newton, 2001*). In the absence of Ca^{2+}, $C2^{WT}$ displayed a characteristic intrinsic fluorescence emission spectrum that peaked around 340 nm (*Figure 2C*, *dark green*). A similar basal emission spectrum was observed for $C2^{D/A}$ (*Figure 2C*, *dark blue*), suggesting that D-to-A mutations did not affect domain folding (*Nalefski and Newton, 2001*). Addition of 1 mM Ca^{2+} increased the fluorescence intensity of $C2^{WT}$ (*Figure 2C*, *light green*) but not $C2^{D/A}$ (*light blue*, *Figure 2C*), indicating that D-to-A mutations prevent Ca^{2+}-dependent rearrangements.

When activated by either phorbol esters or Ca^{2+}, PKC translocates from the cytoplasm to the plasma membrane (*Newton, 2010*). We utilized this property to test the effects of the D-to-A mutations on the response of PKCβ to Ca^{2+} increases. We expressed $PKCβ^{WT}$-YFP or $PKCβ^{D/A}$-YFP in HEK293T cells and monitored the subcellular distribution of the kinase. The Ca^{2+} ionophore ionomycin induced translocation of $PKCβ^{WT}$-YFP (*Figure 2D*, *top left*), but did not alter the intracellular distribution of $PKCβ^{D/A}$-YFP (*Figure 2D*, *top right*). In contrast, PDBu, which binds to the C1 domain, caused both $PKCβ^{WT}$-YFP and $PKCβ^{D/A}$-YFP to translocate. This result indicates that Ca^{2+} binding to the PKC C2 domain is necessary for Ca^{2+}-induced, but not PDBu-induced, translocation of PKCβ. Moreover, it suggests that D-to-A mutations in the C2 domain prevent Ca^{2+} activation of PKCβ without interfering with C1-domain-mediated membrane recruitment of PKCβ.

We next tested whether Ca^{2+} binding to the PKCβ C2 domain is required for PTP. Using AAV to express $PKCβ^{D/A}$-YFP, we found that $PKCβ^{D/A}$-YFP localized to vGlut1-positive areas and distributed similarly to $PKCβ^{WT}$-YFP (*Figure 3A*, compare to *Figure 1E*). Expression of $PKCβ^{D/A}$-YFP in αβ dko calyces, similar to wild-type PKCβ, did not affect basal synaptic properties (*Figure 3—figure supplement 1*, *Figure 3—source data 2*). However, in stark contrast to wild-type PKCβ, $PKCβ^{D/A}$ failed to rescue PTP (*Figure 3B*, *blue*; also see *Figure 3D*, left). The inability of $PKCβ^{D/A}$-YFP to support PTP could be due to a loss of Ca^{2+} binding to PKCβ; alternatively, the D-to-A mutations may have induced more profound impairments of PKCβ, rendering it unable to enhance neurotransmitter release. To distinguish between these possibilities, we tested PDBu-induced potentiation in $PKCβ^{D/A}$-YFP-expressing calyces. Compellingly, PDBu-induced potentiation in $PKCβ^{D/A}$-YFP-expressing calyces was rescued to wild-type levels (*Figure 3C*, *blue*; also see *Figure 3D*, right). This indicates that $PKCβ^{D/A}$-YFP retained its ability to enhance synaptic transmission. We conclude that $PKCβ^{D/A}$-YFP is unable to mediate PTP because it is unable to bind Ca^{2+}, and that Ca^{2+} binding to the C2 domain of PKCβ is required for PTP. Therefore, PKCβ is a Ca^{2+} sensor for PTP.

Discussion

To the best of our knowledge, PKCβ is the first Ca^{2+} sensor to be identified specifically for short-term synaptic plasticity. Similar to synaptotagmin-1, synaptotagmin-2, and synaptotagmin-9, PKCβ requires binding of Ca^{2+} to its C2 domain for its Ca^{2+}-sensing function (*Figure 3*). However, PKCβ acts upstream
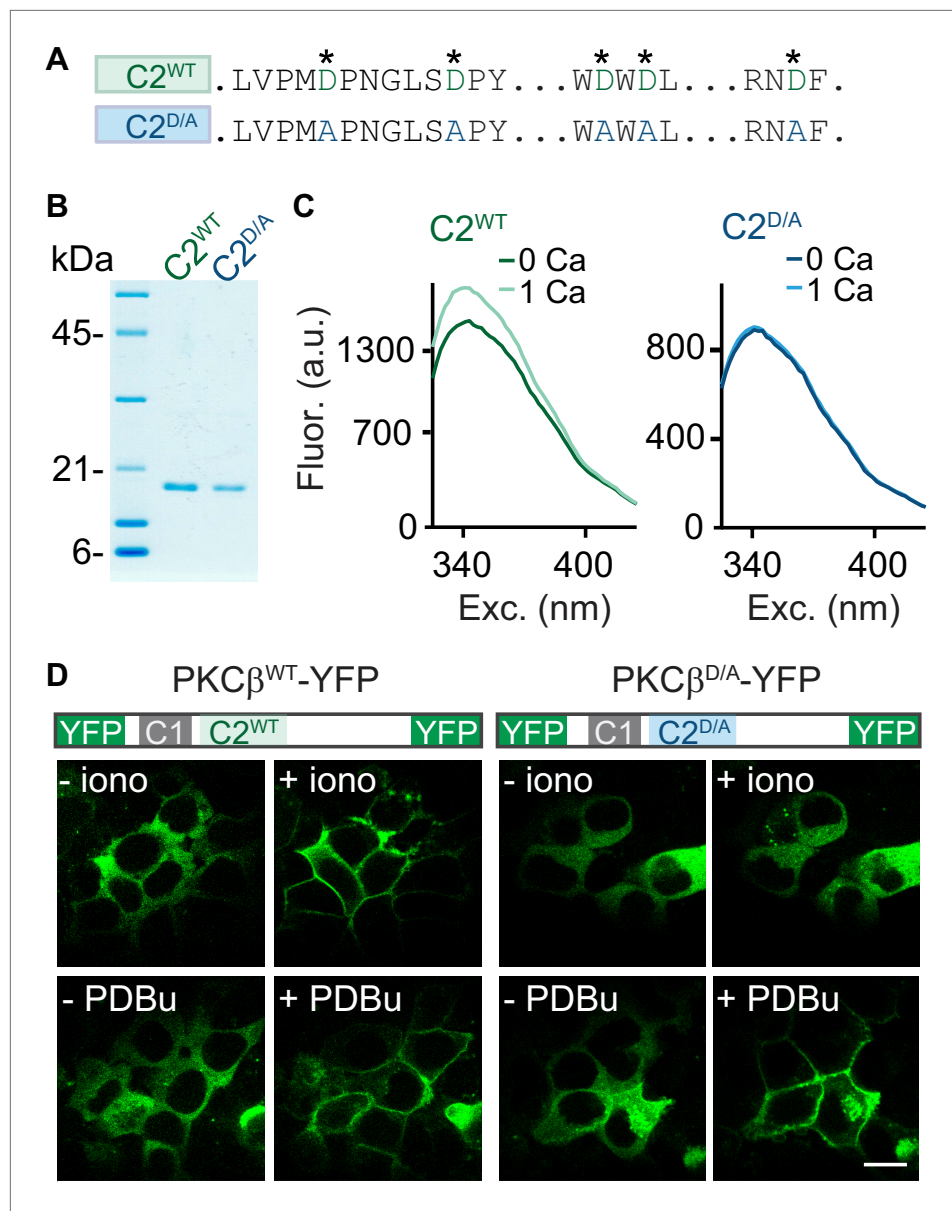
Figure 2. C2-domain mutations of PKCβ abolish Ca²⁺ binding and Ca²⁺-induced translocation without impairing phorbol ester-induced translocation. (**A**) A partial sequence of the PKCβ C2 domain is shown with Ca²⁺-coordinating aspartates in green. These aspartates were mutated to alanines (*blue*) in the C2^D/A construct. Also see ***Figure 2—figure supplement 1***. (**B**) Coomassie blue-stained gel of recombinant wild-type (C2^WT) and mutant (C2^D/A) PKCβ C2 domains. (**C**) Averaged intrinsic tryptophan fluorescence is shown for C2^WT and C2^D/A. Fluorescence emission spectra were recorded in 0 mM Ca²⁺ (*bold traces*) and 1 mM Ca²⁺ (*light traces*). Peak fluorescence intensity change: C2^WT:17 ± 1.3%; C2^D/A: −1.3 ± 2.0%. (**D**) Translocation of PKCβ^WT-YFP (left) and PKCβ^D/A-YFP (right) in HEK293T cells was monitored in response to the Ca²⁺ ionophore ionomycin and in response to PDBu. Ca²⁺ increases caused PKCβ^WT-YFP to translocate, but not PKCβ^D/A-YFP. Both PKCβ^WT-YFP and PKCβ^D/A-YFP translocated in response to PDBu. Scale bar: 10 µm.
DOI: 10.7554/eLife.03011.012

The following figure supplements are available for figure 2:

Figure supplement 1. Protein sequence alignment for PKCβ C2^WT and PKCβ C2^D/A.
DOI: 10.7554/eLife.03011.013

of vesicle fusion (***de Jong and Verhage, 2009***), does not regulate basal transmission or paired-pulse plasticity (***Figure 1—figure supplement 4***), and is not expected to be activated by single stimuli. How do PKCβ and synaptotagmins respond to such different activity patterns and, consequently, such
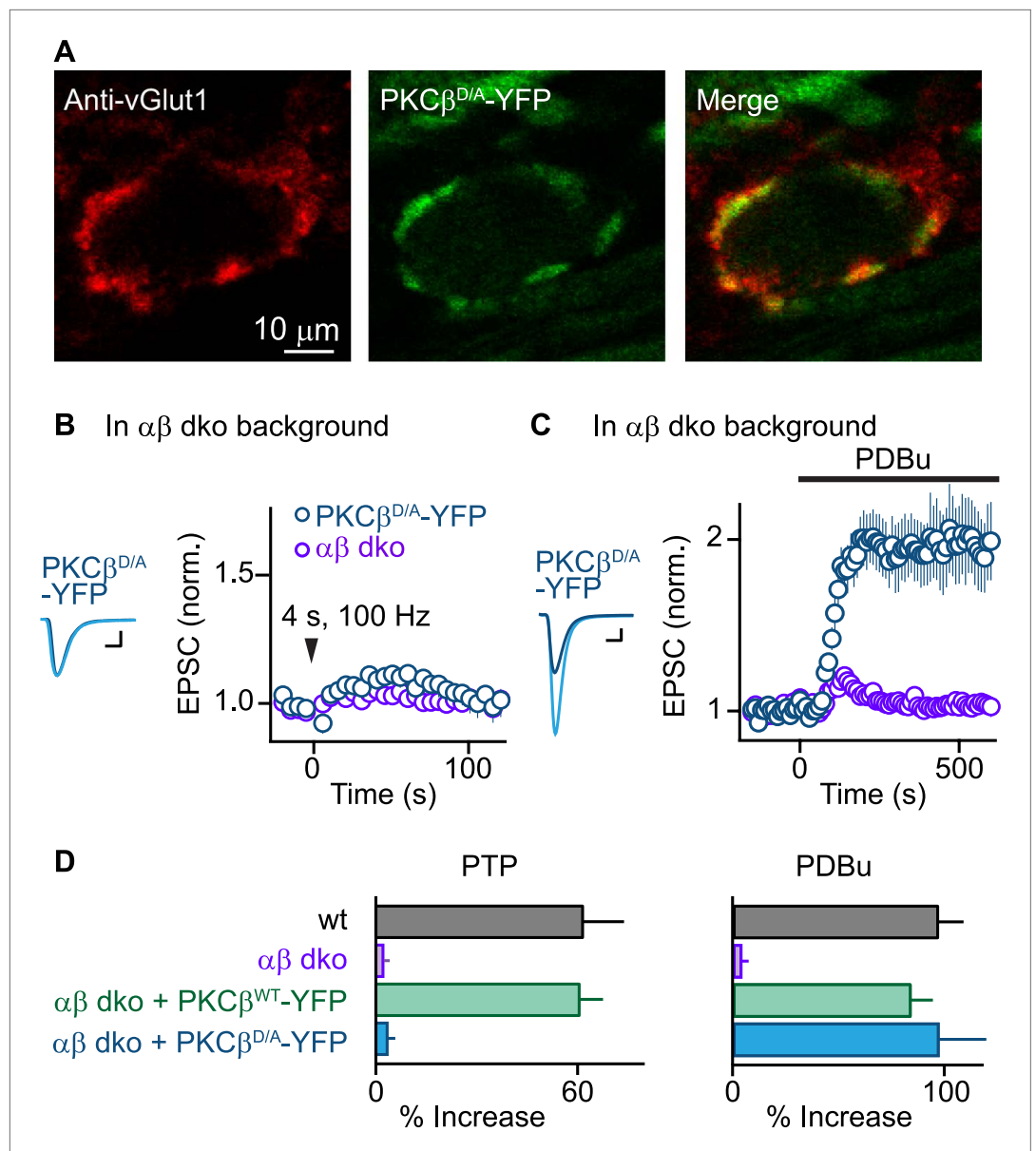
Figure 3. PTP requires Ca²⁺ binding to PKCβ but phorbol ester-induced potentiation does not. (**A**) Confocal images of a brain section labeled with an antibody against vGlut1 (*red*) are shown for a calyx of Held expressing PKCβ^D/A^-YFP (*green*) in a PKCαβ dko animal. (**B** and **C**) Synaptic plasticity was examined in PKCαβ dko animals at calyces of Held expressing Ca²⁺-insensitive PKCβ (PKCβ^D/A^-YFP, *blue traces*). Representative traces and time-courses (mean ± SEM) are shown following tetanic stimulation (**B**) and during bath application of PDBu (**C**). For (**B**), PKCβ^D/A^: 3.6 ± 2.2%; for (**C**), PKCβ^D/A^: 98 ± 23%. Scale bars: 1 nA, 1 ms. In (**B** and **C**), the αβ dko group data from *Figure 1B,C* respectively are re-plotted for comparison. For basal synaptic properties of the PKCβ^D/A^-YFP-expressing group, see *Figure 3—figure supplement 1* and *Figure 3—source data 2*. (**D**) Summary plots (mean ± SEM) of the magnitude of synaptic enhancement produced by tetanic stimulation (left) and by PDBu (right). Source data are provided in *Figure 3—source data 1 and 2*. See also *Figure 1—source data 1 and 2*.
DOI: 10.7554/eLife.03011.014

The following source data and figure supplements are available for figure 3:

Source data 1. Summary and statistical analyses of synaptic properties during PTP and PDBu-induced potentiation.
DOI: 10.7554/eLife.03011.015

Source data 2. Summary and statistical analyses of basal synaptic properties.
DOI: 10.7554/eLife.03011.016

Figure supplement 1. Basal synaptic properties are not altered by PKCβ^D/A^-YFP expression.
DOI: 10.7554/eLife.03011.017

different Ca^{2+} signals? It is likely a combination of differences in Ca^{2+}-binding properties and subcellular localization that underlie these contrasting responses (*Nalefski et al., 2001*). Synaptotagmin-1 binds Ca^{2+} cooperatively with low affinity and fast kinetics, and localizes close to release sites on synaptic vesicles; therefore, it is poised to detect large, transient Ca^{2+} signals near open voltage-gated Ca^{2+} channels (*Sudhof, 2013*). In contrast, PKCβ is activated by lower Ca^{2+} levels with lower cooperativity and is cytosolic (*Nalefski and Newton, 2001*; *Kohout et al., 2002*). Prolonged stimulation is necessary to produce a sufficient buildup of Ca^{2+} to activate PKCβ, which is consistent with the prolonged activity requirement for PTP (*Habets and Borst, 2005*; *Korogod et al., 2005*).

It is unlikely that PKCβ is the sole Ca^{2+} sensor that triggers PTP. At the granule cell to Purkinje cell synapse, PTP can be dependent on either PKCα or PKCβ (*Fioravante et al., 2012*), and at the calyx of Held synapse prior to the onset of hearing PTP depends on PKCγ (*Chu et al., 2014*). These findings suggest that Ca^{2+}-sensitive PKC isoforms, including PKCα and PKCγ, may constitute a class of proteins that acts as Ca^{2+} sensors for PTP, much as multiple isoforms of synaptotagmin act as Ca^{2+} sensors for fast synaptic transmission (*Sudhof, 2012*). Further studies are required to determine whether PKCα, PKCγ, and other Ca^{2+}-sensitive proteins implicated in PTP, such as Munc13 (*Wierda et al., 2007*), calmodulin (*Junge et al., 2004*), and synaptotagmin-2 (*He et al., 2009*; *Xue and Wu, 2010*), can also act as Ca^{2+} sensors to produce PTP.

PKCβ mediates PTP by phosphorylating downstream targets (*Genç et al., 2014*), which could explain how PTP outlives elevations of presynaptic Ca^{2+} (*Fioravante and Regehr, 2011*). We suggest that PKCβ is a founding member of a new class of Ca^{2+} sensors that function upstream of vesicle fusion to regulate short-term plasticity.

Materials and methods

DNA constructs and viruses

Cloning was performed by Genscript. Viruses were generated by the University of Pennsylvania Vector Core. All constructs were verified by sequencing. Wild-type PKCβ-YFP (β^{WT}-YFP) was obtained through PCR from Addgene plasmid #14866 (*Violin et al., 2003*), using the following primers: 5'-GACACAACAGTCTCGAACTTAATCGAACCCGCGGCACGAGCCTCGACG-3'; 3'-GGGAAAAAGA TCGGATCCTCAGGCGTCGACGGGCCCTCTAGATTACTTG-5'. To generate an adeno-associated viral vector, PKCβ^WT^-YFP was inserted into a pENN.AAV.CMV.TurboRFP.RBG cis-plasmid (courtesy of the University of Pennsylvania Vector Core) using SacII and SalI, after removal of the TurboRFP sequence with SpeI and XhoI. Mutant PKCβ-YFP ($\beta^{D/A}$-YFP) was generated by replacing the 5 aspartates that coordinate calcium binding (*Sutton and Sprang, 1998*) with alanines through PCR.

To generate bacterial expression plasmids of the PKCβ C2 domain, the sequences for C2^WT^ or C2^D/A^ (a.a. 157–294) (*Torrecillas et al., 2003*) (see also *Figure 2—figure supplement 1*) were inserted into a pGEX-KG vector (Addgene database #2890) using XbaI and NcoI and the following primers: 5'-TCCGGTGGTGGTGGTGGAATTCTAGAAGAACGCCGTGGCCGCATC-3' and 3'-AAGCTTGAGCTC GAGTCGACCCATGGTCATCCTTCCGGCGGCACCG-5'.

Animals

All animal experiments were conducted at Harvard Medical School and were completed in accordance with guidelines by the Harvard Medical Area Standing Committee on Animals. PKCαβ double knockout (dko) mice were obtained through breeding of PKCα and PKCβ single knockout (ko) animals generated by M Leitges (*Leitges et al., 1996*, *2002*). The probability of obtaining an αβ double knockout animal from heterologous (het) crosses is very low (1:16), making viral injection experiments unfeasible. We therefore bred het-ko animals together to increase the probability of getting desired animals. Similarly, to increase the probability of obtaining wild-type mice, we crossed PKC het–het or het-wild-type mice to use as wild-type controls. Wild-type mice were derived from the same genetic line as αβ dko animals. To prevent genetic drift in the inbred ko lines, we backcrossed them every second generation to C57BL/6J or 129S2. For experiments, animals of both sexes were used and age-matched wild-type, PKCα ko and PKCαβ dko mice from our colony were interleaved.

Surgery

P4 pups were stereotactically and unilaterally injected under isofluorane anesthesia with AAVs into the VCn (from lambda: 1.3 mm lateral, 0.9 mm caudal, 3 mm ventral), where globular bushy cells that give rise to calyx of Held synapses in the contralateral MNTB reside. Injections (600 nl at a rate of 1 nl/s)

were performed with an UltraMicroPump (UMP3, WPI, Sarasota FL) and Wiretrol II capillary micropipettes (Drummond Scientific, Broomall PA) pulled to a fine tip (10–20 μm diameter). At this age, the skull is sufficiently soft so it can be penetrated with a $28^1/_2$–gage needle without the need for drilling. After the injection, the skin was closed with Gluture (Abbott Laboratories, Irving TX), and pups were allowed to recover on a heating pad prior to returning to the home cage. 14–18 days were allowed for expression prior to slice preparation.

Preparation of brain slices

The calyx of Held synapse in the auditory brainstem was chosen for this study because of its monosynaptic innervation and its amenability to viral manipulations. Indeed, our study would not be possible at more 'conventional' polysynaptic preparations such as the CA3-CA1 hippocampal synapse because it is not possible to infect 100% of synapses with viruses. Transverse 190-μm to 200-μm-thick brainstem slices containing the MNTB were made with a vibratome slicer (VT1000S, Leica, Buffalo Grove IL) from juvenile (postnatal day 17–22) mice deeply anesthetized with isoflurane. Brains were dissected and sliced at 4°C in cutting solution consisting of the following (in mM): 125 NaCl, 25 $NaHCO_3$, 1.25 NaH_2PO_4, 2.5 KCl, 0.1 $CaCl_2$, 3 $MgCl_2$, 25 glucose, 3 myo-inositol, 2 Na-pyruvate, 0.4 ascorbic acid, continuously bubbled with 95% O_2/5% CO_2 (pH 7.4). Slices were incubated at 32°C for 30 min in a bicarbonate-buffered solution composed of the following (in mM): 125 NaCl, 25 $NaHCO_3$, 1.25 NaH_2PO_4, 2.5 KCl, 2 $CaCl_2$, 1 $MgCl_2$, 25 glucose, 3 myo-inositol, 2 Na-pyruvate, 0.4 ascorbic acid, continuously bubbled with 95% O_2/5% CO_2 (pH 7.4).

Electrophysiology

Slices were transferred to a recording chamber at room temperature (21–24°C) under an upright microscope (Olympus, Center Valley PA) equipped with a 60× objective. During recordings, the standard perfusion solution consisted of the bicarbonate-buffered solution (see above) with 1 μM strychnine and 25 μM bicuculline (R&D Systems, Minneapolis MN) to block inhibition. Slices were superfused at 1–3 ml/min with this external solution. Whole-cell postsynaptic patch-clamp recordings were made from visually identified cells in the MNTB region using glass pipettes of 2–3 MΩ resistance, filled with an internal recording solution of the following (in mM): 20 CsCl, 140 Cs-gluconate, 20 TEA-Cl, 10 HEPES, 5 EGTA, 5 Na_2-phosphocreatine, 4 ATP-Mg, 0.3 GTP-Na. Series resistance (R_s) was compensated by up to 70%, and the membrane potential was held at −70 mV.

EPSCs were evoked by stimulating presynaptic axons with a custom-made bipolar stimulating electrode midway between the medial border of the MNTB and the midline of the brainstem. For slice recordings from injected animals, principal neurons in the MNTB contralateral to the injection site were selected based on the presence of YFP-expressing presynaptic terminals. A Multiclamp 700B (Axon Instruments/Molecular Devices, Sunnyvale CA) amplifier was used. Recordings were digitized at 20 KHz with an ITC-18 A/D converter (Instrutech Corp./HEKA Elektronik, Bellmore NY) using custom macros (written by MA Xu-Friedman) in Igor Pro (Wavemetrics, Portland OR) and filtered at 8 kHz. Macros can be found on Dr Xu-Friedman's website http://biology.buffalo.edu/Faculty/Xu_Friedman/mafPC/sign_in.html.

The protocol for inducing PTP was as follows: an estimate of baseline synaptic strength was obtained through low-frequency stimulation at 0.2 Hz for 25 s. PTP was induced with a 4-s stimulus train at 100 Hz, followed by low-frequency stimulation to test for PTP. For phorbol ester experiments, PDBu (1 μM; Tocris, UK) was washed in for 10 min once a stable baseline of at least 3 min was established. Synaptic strength was evaluated by afferent fiber stimuli, repeated every 20 s. During the intertrial intervals, 5 s stretches of postsynaptic current were recorded to assess the frequency and amplitude of mEPSCs. To assess PPR, pulses were delivered at an inter-stimulus interval of 10 ms. For all recordings, the access resistance and leak current were monitored, and experiments were rejected if either of these parameters changed significantly.

Data analysis

Data analysis was performed using routines written in IgorPro (WaveMetrics). PTP magnitude was calculated as the ratio of EPSC amplitude 10 s after the 4-s, 100 Hz train over the average baseline. The magnitude of PDBu-induced potentiation was estimated by averaging the steady-state responses, 430–600 s from wash-in onset. To analyze spontaneous events, mEPSCs were detected using a threshold (average peak to peak noise in the baseline) of the first derivative of the raw current trace and confirmed visually. Statistical analyses were done using one-way ANOVA tests for multiple group comparisons followed by Tukey post-hoc analysis, or Kruskal–Wallis non-parametric ANOVA for data sets

that were not normally distributed. Pairwise comparisons were performed with Student's t tests. Level of significance was set at $p<0.05$.

To determine the contributions of RRP and p to wild-type and rescued PTP, stimulus trains were used in the presence of kynurenate (1 mM) and CTZ (0.1 mM) to prevent postsynaptic receptor saturation and desensitization. Briefly, the amplitude of the first 40 responses to the stimulus train used to induce PTP and to a stimulus train (400 ms, 100 Hz) 10 s later (at the peak of PTP) were measured, and a plot of the cumulative EPSC for each train vs the stimulus number was made. The key to this approach is that the EPSC amplitude eventually reaches a steady-state level, and under these conditions the RRP is depleted and the remaining release is due to replenishment from a recycling/reserve pool (*Schneggenburger et al., 1999*). The size of the RRP can then be determined by a linear fit to the steady-state responses (last 15 EPSCs), which is extrapolated back to the y-axis (*Moulder and Mennerick, 2005*; *Thanawala and Regehr, 2013*). p is then calculated from EPSC1/RRP.

Immunohistochemistry

150-µm thick transverse brainstem slices were prepared as described above from P18–P22 animals injected with AAVs and fixed with 4% paraformaldehyde for 2 hr at 4°C. At the end of fixation, slices were transferred to phosphate buffered saline (Sigma-Aldrich, St. Louis MO) and stored at 4°C until further processing. Slices were then incubated in blocking solution (phosphate buffered saline +0.25% Triton X-100 [PBST] +10% normal goat serum) for 1 hr at room temperature. Slices were incubated with primary antibody (anti-vGlut1 guinea pig polyclonal [Synaptic Systems, Germany]) in PBST overnight at 4°C, followed by incubation with secondary antibody (goat anti-guinea pig Alexa 568-conjugated [Life Technologies, Carlsbad CA]) in PBST for 2 hr. Slices were mounted to Superfrost glass slides (VWR, Visalia CA) and air-dried for 30 min. Following application of Prolong anti-fade medium (Invitrogen), slices were covered with a top glass coverslip (VWR) and allowed to dry for 24 hr prior to imaging. Antibodies were used at 1:500 dilution.

Images were acquired with a Zeiss 510 Meta confocal microscope using a Plan-apochromat 1.4 NA 63x oil lens. Emission filters were BP570-670 nm for the red channel (vGlut1) and BP500-550 for YFP (PKCβ). Single optical sections at 1024 × 1024 (average of three scans) were obtained sequentially for the different channels. Color channels were split and merged in ImageJ to obtain the composite images in RGB.

Protein purification

N-terminal GST fusion proteins of PKCβ C2^{WT} and C2$^{D/A}$ were expressed in *Escherichia coli* BL21 cells. Pelleted bacteria were resuspended in ice-cold PBS supplemented with 500 µM EDTA, 0.5 mg/ml lysozyme (Amresco, Solon OH), and protease inhibitor cocktail (Easypack; Roche, South San Francisco CA), and the bacteria were lysed by sonication. After centrifugation at 11,200 RPM for 30 min, the soluble fraction was collected and incubated with glutathione sepharose 4B beads (GE healthcare, Pittsburgh PA) for 1 hr at 4°C. Samples were cleared from nucleic acid contaminants with benzonase (40 U/ml, Sigma) for 3 hr at RT, and subsequently eluted from the beads with solution containing 100 mM Tris, 10 mM CaCl$_2$, 5 mM Glutathione (pH 7.4) for 1 hr at 4°C. GST was cleaved with thrombin-agarose (100 µl resin/mg protein, Sigma) for 24 hr at 4°C, and samples were dialyzed to solution containing 40 mM Tris–HCl pH 7.4, 100 mM NaCl, and 0.5 mM Na-EGTA. GST was removed from the samples using glutathione sepharose 4B beads. 10 µl of purified protein was run on a 12% SDS gel and Coomassie blue-stained to check for purity (*Figure 2B*).

Intrinsic tryptophan fluorescence assay

Intrinsic tryptophan fluorescence of purified recombinant C2^{WT} and C2$^{D/A}$ was monitored in dialysis buffer (see above). Emission spectra were recorded from 325 to 425 nm on a Spectramax M5 microplate reader (Molecular Devices). Excitation was set at 295 nm and peak intrinsic fluorescence change (ΔF) upon addition of 1 mM free Ca^{2+} was estimated at 341 nm. To correct for the effect of volume increase on fluorescence readings upon addition of Ca^{2+}-containing buffer, ΔF in buffer-alone controls was subtracted from fluorescence values in buffer+Ca^{2+} groups. Experiments were repeated with two independently purified batches of protein, for a total of seven times. Similar results were obtained every time.

Protein translocation assay

HEK293T cells plated on glass coverslips were transfected with PKCβ^{WT}-YFP or β$^{D/A}$-YFP expression vectors using Lipofectamine 2000 (Life Technologies). 24 hr after transfection, the coverslips were transferred to the imaging chamber of a custom-built 2-photon laser scanning microscope system and

superfused with buffer (138 mM NaCl, 1.5 mM KCl, 10 mM HEPES, 1 mM $MgCl_2$, 2 mM $CaCl_2$, 10 mM glucose, pH 7.4) at 2 ml/min. YFP was excited at 840 nm with a Ti-Sapphire laser through a 60×, 1.1 NA water-immersion Olympus lens. A 500–550 BP emission filter was used. 512 × 512 frame scans were acquired at a rate of 1 line/4 ms, every 30 s. To stimulate translocation, the superfusion solution was switched to one containing 1 µM PDBu or 10 µM ionomycin (R&D Systems) for 15 min. The experiment was repeated three times for PKCβ[WT]-YFP and twice for PKCβ[D/A]-YFP, with similar results. Acquired images were exported to ImageJ and brightness/contrast was adjusted equally for all images within an experiment for display purposes.

Acknowledgements

Additional information

Author contributions

DF, Conception and design, Acquisition of data, Analysis and interpretation of data, Drafting or revising the article; YXC, APHJ, Acquisition of data, Analysis and interpretation of data, Drafting or revising the article; ML, Generated PKCα and PKCβ knockout mice, Provided expertise on PKC signaling, Contributed unpublished essential data or reagents; PSK, WGR, Conception and design, Analysis and interpretation of data, Drafting or revising the article

Ethics

Animal experimentation: Animal experimentation: All procedures involving animals were performed in accordance with the guidelines of the National Institutes of Health. The protocol used (1493) was approved by the Harvard Medical Area (HMA) standing committee on animals.

References

Abbott LF, Regehr WG. 2004. Synaptic computation. *Nature* **431**:796–803. doi: 10.1038/nature03010.

Brager DH, Cai X, Thompson SM. 2003. Activity-dependent activation of presynaptic protein kinase C mediates post-tetanic potentiation. *Nature Neuroscience* **6**:551–552. doi: 10.1038/nn1067.

Brose N, Rosenmund C. 2002. Move over protein kinase C, you've got company: alternative cellular effectors of diacylglycerol and phorbol esters. *Journal of Cell Science* **115**:4399–4411. doi: 10.1242/jcs.00122.

Chu Y, Fioravante D, Leitges M, Regehr WG. 2014. Calcium-dependent PKC isoforms have specialized roles in short-term synaptic plasticity. *Neuron* **82**:859–871. doi: 10.1016/j.neuron.2014.04.003.

de Jong AP, Verhage M. 2009. Presynaptic signal transduction pathways that modulate synaptic transmission. *Current Opinion in Neurobiology* **19**:245–253. doi: 10.1016/j.conb.2009.06.005.

Fedchyshyn MJ, Wang LY. 2005. Developmental transformation of the release modality at the calyx of Held synapse. *The Journal of Neuroscience* **25**:4131–4140. doi: 10.1523/JNEUROSCI.0350-05.2005.

Fioravante D, Chu Y, Myoga MH, Leitges M, Regehr WG. 2011. Calcium-dependent isoforms of protein kinase C mediate posttetanic potentiation at the calyx of Held. *Neuron* **70**:1005–1019. doi: 10.1016/j.neuron.2011.04.019.

Fioravante D, Myoga MH, Leitges M, Regehr WG. 2012. Adaptive regulation maintains posttetanic potentiation at cerebellar granule cell synapses in the absence of calcium-dependent PKC. *The Journal of Neuroscience* **32**:13004–13009. doi: 10.1523/JNEUROSCI.0683-12.2012.

Fioravante D, Regehr WG. 2011. Short-term forms of presynaptic plasticity. *Current Opinion in Neurobiology* **21**:269–274. doi: 10.1016/j.conb.2011.02.003.

Genç O, Kochubey O, Toonen RF, Verhage M, Schneggenburger R. 2014. Munc18-1 is a dynamically regulated PKC target during short-term enhancement of transmitter release. *eLife* **3**:e01715. doi: 10.7554/eLife.01715.

Groffen AJ, Martens S, Diez Arazola R, Cornelisse LN, Lozovaya N, de Jong AP, Goriounova NA, Habets RL, Takai Y, Borst JG, Brose N, McMahon HT, Verhage M. 2010. Doc2b is a high-affinity Ca2+ sensor for spontaneous neurotransmitter release. *Science* **327**:1614–1618. doi: 10.1126/science.1183765.

Habets RL, Borst JG. 2005. Post-tetanic potentiation in the rat calyx of Held synapse. *The Journal of Physiology* **564**:173–187. doi: 10.1113/jphysiol.2004.079160.

Habets RL, Borst JG. 2007. Dynamics of the readily releasable pool during post-tetanic potentiation in the rat calyx of Held synapse. *The Journal of Physiology* **581**:467–478. doi: 10.1113/jphysiol.2006.127365.

He L, Xue L, Xu J, McNeil BD, Bai L, Melicoff E, Adachi R, Wu LG. 2009. Compound vesicle fusion increases quantal size and potentiates synaptic transmission. *Nature* **459**:93–97. doi: 10.1038/nature07860.

Junge HJ, Rhee JS, Jahn O, Varoqueaux F, Spiess J, Waxham MN, Rosenmund C, Brose N. 2004. Calmodulin and Munc13 form a Ca2+ sensor/effector complex that controls short-term synaptic plasticity. *Cell* **118**:389–401. doi: 10.1016/j.cell.2004.06.029.

Kaeser PS, Regehr WG. 2013. Molecular mechanisms for synchronous, asynchronous, and spontaneous neurotransmitter release. *Annual Review of Physiology* **76**:333–363. doi: 10.1146/annurev-physiol-021113-170338.

Kohout SC, Corbalan-Garcia S, Torrecillas A, Gomez-Fernandez JC, Falke JJ. 2002. C2 domains of protein kinase C isoforms alpha, beta, and gamma: activation parameters and calcium stoichiometries of the membrane-bound state. *Biochemistry* **41**:11411–11424. doi: 10.1021/bi026041k.

Korogod N, Lou X, Schneggenburger R. 2005. Presynaptic Ca2+ requirements and developmental regulation of posttetanic potentiation at the calyx of Held. *The Journal of Neuroscience* **25**:5127–5137. doi: 10.1523/JNEUROSCI.1295-05.2005.

Leitges M, Plomann M, Standaert ML, Bandyopadhyay G, Sajan MP, Kanoh Y, Farese RV. 2002. Knockout of PKC alpha enhances insulin signaling through PI3K. *Molecular Endocrinology* **16**:847–858. doi: 10.1210/mend.16.4.0809.

Leitges M, Schmedt C, Guinamard R, Davoust J, Schaal S, Stabel S, Tarakhovsky A. 1996. Immunodeficiency in protein kinase cbeta-deficient mice. *Science* **273**:788–791. doi: 10.1126/science.273.5276.788.

Mochida S, Few AP, Scheuer T, Catterall WA. 2008. Regulation of presynaptic Ca(V)2.1 channels by Ca2+ sensor proteins mediates short-term synaptic plasticity. *Neuron* **57**:210–216. doi: 10.1016/j.neuron.2007.11.036.

Moulder KL, Mennerick S. 2005. Reluctant vesicles contribute to the total readily releasable pool in glutamatergic hippocampal neurons. *The Journal of Neuroscience* **25**:3842–3850. doi: 10.1523/JNEUROSCI.5231-04.2005.

Nalefski EA, Falke JJ. 1996. The C2 domain calcium-binding motif: structural and functional diversity. *Protein Science* **5**:2375–2390. doi: 10.1002/pro.5560051201.

Nalefski EA, Newton AC. 2001. Membrane binding kinetics of protein kinase betaII mediated by the C2 domain. *Biochemistry* **40**:13216–13229. doi: 10.1021/bi010761u.

Nalefski EA, Wisner MA, Chen JZ, Sprang SR, Fukuda M, Mikoshiba K, Falke JJ. 2001. C2 domains from different Ca2+ signaling pathways display functional and mechanistic diversity. *Biochemistry* **40**:3089–3100. doi: 10.1021/bi001968a.

Newton AC. 2010. Protein kinase C: poised to signal. *American Journal of Physiology Endocrinology and Metabolism* **298**:E395–E402. doi: 10.1152/ajpendo.00477.2009.

Pang ZP, Bacaj T, Yang X, Zhou P, Xu W, Sudhof TC. 2011. Doc2 supports spontaneous synaptic transmission by a Ca(2+)-independent mechanism. *Neuron* **70**:244–251. doi: 10.1016/j.neuron.2011.03.011.

Regehr WG, Delaney KR, Tank DW. 1994. The role of presynaptic calcium in short-term enhancement at the hippocampal mossy fiber synapse. *The Journal of Neuroscience* **14**:523–537.

Saitoh N, Hori T, Takahashi T. 2001. Activation of the epsilon isoform of protein kinase C in the mammalian nerve terminal. *Proceedings of the National Academy of Sciences of the United States of America* **98**:14017–14021. doi: 10.1073/pnas.241333598.

Sakaba T, Neher E. 2001. Calmodulin mediates rapid recruitment of fast-releasing synaptic vesicles at a calyx-type synapse. *Neuron* **32**:1119–1131. doi: 10.1016/S0896-6273(01)00543-8.

Schneggenburger R, Meyer AC, Neher E. 1999. Released fraction and total size of a pool of immediately available transmitter quanta at a calyx synapse. *Neuron* **23**:399–409. doi: 10.1016/S0896-6273(00)80789-8.

Shao X, Davletov BA, Sutton RB, Sudhof TC, Rizo J. 1996. Bipartite Ca2+-binding motif in C2 domains of synaptotagmin and protein kinase C. *Science* **273**:248–251. doi: 10.1126/science.273.5272.248.

Shin OH, Lu J, Rhee JS, Tomchick DR, Pang ZP, Wojcik SM, Camacho-Perez M, Brose N, Machius M, Rizo J, Rosenmund C, Sudhof TC. 2010. Munc13 C2B domain is an activity-dependent Ca2+ regulator of synaptic exocytosis. *Nature Structural & Molecular Biology* **17**:280–288. doi: 10.1038/nsmb.1758.

Silva AJ, Rosahl TW, Chapman PF, Marowitz Z, Friedman E, Frankland PW, Cestari V, Cioffi D, Sudhof TC, Bourtchuladze R. 1996. Impaired learning in mice with abnormal short-lived plasticity. *Current Biology* **6**:1509–1518. doi: 10.1016/S0960-9822(96)00756-7.

Sonntag M, Englitz B, Kopp-Scheinpflug C, Rubsamen R. 2009. Early postnatal development of spontaneous and acoustically evoked discharge activity of principal cells of the medial nucleus of the trapezoid body: an in vivo study in mice. *The Journal of Neuroscience* **29**:9510–9520. doi: 10.1523/JNEUROSCI.1377-09.2009.

Sudhof TC. 2012. Calcium control of neurotransmitter release. *Cold Spring Harbour Perspectives in Biology* **4**:a011353. doi: 10.1101/cshperspect.a011353.

Sudhof TC. 2013. Neurotransmitter release: the last millisecond in the life of a synaptic vesicle. *Neuron* **80**: 675–690. doi: 10.1016/j.neuron.2013.10.022.

Sutton RB, Sprang SR. 1998. Structure of the protein kinase Cbeta phospholipid-binding C2 domain complexed with Ca2+. *Structure* **6**:1395–1405. doi: 10.1016/S0969-2126(98)00139-7.

Tanaka M, Sagawa S, Hoshi J, Shimoma F, Matsuda I, Sakoda K, Sasase T, Shindo M, Inaba T. 2004. Synthesis of anilino-monoindolylmaleimides as potent and selective PKCbeta inhibitors. *Bioorganic & Medicinal Chemistry Letters* **14**:5171–5174. doi: 10.1016/j.bmcl.2004.07.061.

Thanawala MS, Regehr WG. 2013. Presynaptic calcium influx controls neurotransmitter release in part by regulating the effective size of the readily releasable pool. *The Journal of Neuroscience* **33**:4625–4633. doi: 10.1523/JNEUROSCI.4031-12.2013.

Torrecillas A, Corbalan-Garcia S, Gomez-Fernandez JC. 2003. Structural study of the C2 domains of the classical PKC isoenzymes using infrared spectroscopy and two-dimensional infrared correlation spectroscopy. *Biochemistry* **42**:11669–11681. doi: 10.1021/bi034759+.

Ubach J, Zhang X, Shao X, Sudhof TC, Rizo J. 1998. Ca2+ binding to synaptotagmin: how many Ca2+ ions bind to the tip of a C2-domain? *The EMBO Journal* **17**:3921–3930. doi: 10.1093/emboj/17.14.3921.

Violin JD, Zhang J, Tsien RY, Newton AC. 2003. A genetically encoded fluorescent reporter reveals oscillatory phosphorylation by protein kinase C. *The Journal of Cell Biology* **161**:899–909. doi: 10.1083/jcb.200302125.

Wierda KD, Toonen RF, de Wit H, Brussaard AB, Verhage M. 2007. Interdependence of PKC-dependent and PKC-independent pathways for presynaptic plasticity. *Neuron* **54**:275–290. doi: 10.1016/j.neuron.2007.04.001.

Xue L, Wu LG. 2010. Post-tetanic potentiation is caused by two signalling mechanisms affecting quantal size and quantal content. *The Journal of Physiology* **588**:4987–4994. doi: 10.1113/jphysiol.2010.196964.

Yang YM, Fedchyshyn MJ, Grande G, Aitoubah J, Tsang CW, Xie H, Ackerley CA, Trimble WS, Wang LY. 2010. Septins regulate developmental switching from microdomain to nanodomain coupling of Ca(2+) influx to neurotransmitter release at a central synapse. *Neuron* **67**:100–115. doi: 10.1016/j.neuron.2010.06.003.